J. Fluid Mech. (1999), *vol.* 392, *pp.* 45–71. Printed in the United Kingdom

Turbulent dispersion in a non-homogeneous field

By ILIAS ILIOPOULOS AND THOMAS J. HANRATTY

Department of Chemical Engineering, University of Illinois, Urbana, IL 61801 USA

(Received 19 January 1998 and in revised form 9 February 1999)

Dispersion of fluid particles in non-homogeneous turbulence was studied for fully developed flow in a channel. A point source at a distance of 40 wall units from the wall is considered. Data obtained by carrying out experiments in a direct numerical simulation (DNS) are used to test a stochastic model which utilized a modified Langevin equation. All of the parameters, with the exception of the time scales, are obtained from Eulerian statistics. Good agreement is obtained by making simple assumptions about the spatial variation of the time scales.

1. Introduction

The physics of turbulent transport of heat and mass emerges in a more natural way by using a Lagrangian, rather than an Eulerian, approach. Such an analysis has been exploited for turbulent heat transfer in a rectangular channel in which one wall is heated and one is cooled (Hanratty 1956, 1958; Hanratty & Flint 1958; Eckelman & Hanratty 1972; Papavassiliou & Hanratty 1997). The temperature field was calculated by representing the heated wall as a series of sources and the cold wall as a series of sinks. The results show that the spatial variation of turbulent diffusion coefficients defined in an Eulerian framework are, to a large extent, a manifestation of the time-dependence of diffusion from a line source. Furthermore, Papavassiliou & Hanratty (1995, 1997) have shown that time-averaged temperature fields can be calculated with Lagrangian techniques, for arbitrarily large Prandtl numbers, from the turbulent velocity field given by a direct numerical simulation (DNS).

Two problems that exist in exploiting these methods are addressed in this paper: (i) measurements of Lagrangian statistics are not as plentiful as measurements of Eulerian statistics; (ii) a theoretical method to represent the behaviour of a source or sink needs to be established. Results from a study of the dispersion of fluid particles in a DNS of fully developed turbulent flow in a channel are presented. The source is located at the edge of the viscous wall layer to emphasize the influence of non-homogeneities in the turbulent field. These results are interpreted with a modified Langevin equation.

The classical papers by Taylor (1921, 1935) describe the statistical behaviour of a large number of particles originating from a point source in a homogeneous isotropic turbulent field. The time variation of the mean-squared displacements along one coordinate, $\overline{x_i^2}$, is calculated in terms of a Lagrangian correlation coefficient and the mean-square of a component of the turbulent velocity fluctuations, $\overline{u_i^2}$. For large times $\overline{x_i^2}$ varies linearly with time and the turbulent diffusion coefficient, $E = \frac{1}{2}\mathrm{d}\overline{x_i^2}/\mathrm{d}t$, is found to be equal to $\overline{u_i^2}\tau_L$ where τ_L is the Lagrangian time scale, equal to the area

under the curve defining the Lagrangian correlation coefficient. For smaller times, E is a function of time. For most turbulent flows, the fluctuating velocity field is non-homogeneous and anisotropic, and the time-mean velocity varies with spatial location; the application of Taylor's theory is not clear-cut. One approach is to use stochastic methods to calculate possible paths of particles and to average over a large number of these paths.

Langevin developed a treatment of Brownian motion which considers the change of the velocity of a particle with time as due to a damping force that is proportional to the velocity and a random force which has a zero mean and is uncorrelated for successive times that are arbitrarily close together. Obukhov (1959) applied this concept to turbulent fluid motions and proposed a stochastic differential equation to model dispersion of particles in a homogeneous flow. A consideration of the average behaviour of a large number of particle paths gives the same result as Taylor's analysis if the Lagrangian correlation is represented by $\exp(-t/\tau_L)$.

The Langevin equation can be written in the following form to define a possible change of a component of the velocity of a fluid particle in a homogeneous isotropic field over a time interval $\mathrm{d}t$:

$$\mathrm{d}u_i = -\frac{u_i}{\tau}\mathrm{d}t + \alpha^{1/2}\mathrm{d}\omega, \tag{1}$$

$$\frac{\mathrm{d}x_i}{\mathrm{d}t} = u_i, \tag{2}$$

where u_i identifies the velocity component in the i-direction. In all equations, the tensor convention of summing over repeated indices is not followed. The first term in (1) is deterministic. It represents the persistence of the motion of the fluid particle. The term $\mathrm{d}\omega$ is a sequence of random numbers, with a variance $\langle \mathrm{d}\omega^2 \rangle = \mathrm{d}t$, which is uncorrelated in successive time intervals (a Markovian assumption). The brackets indicate an ensemble average.

The Markovian assumption is not exact. It is a reasonable approximation for the acceleration, which has small correlation times. It is not appropriate for the velocities or positions of the particle. Furthermore, it cannot represent accelerations in the limit of $t \to 0$. Its usefulness can be determined only by comparisons with experiments. Equation (1) can be solved to obtain $\langle u_i^2 \rangle$ for particles which originate from $x_i = x_{i0}$ with a velocity $u_i(0)$ at $t = 0$. In homogeneous turbulence $\langle u_i^2 \rangle = \langle u_i^2(0) \rangle$. This requires that $\alpha = 2\sigma^2/\tau$, where $\sigma^2 = \overline{u_i^2}$ is the mean square of a component of the velocity fluctuations in an Eulerian framework and $\overline{u_i^2} = \langle u_i^2 \rangle$. The constant τ is found to be equal to the Lagrangian time scale, τ_L.

A number of investigators have explored the application of (1) to a non-homogeneous field by allowing σ_i and τ_i to be functions of location and to be different in different directions. Hall (1975) and Reid (1979) obtained satisfactory solutions of (1) and (2) for a constant σ_i and a spatially varying τ_i. They considered dispersion downstream of a ground level source (which was at the bottom of the log-layer). Hall assumed that $\sigma_2 = 1.3u_*$, that τ_2 is proportional to the Eulerian time scale, τ_E, and that the dispersing particles remain in the log-layer, where u_* is the friction velocity and subscript 2 indicates the velocity component perpendicular to the boundary. This assumption leads to the suggestion that $\tau_2 = c\,x_2/U_1$, where c is a constant, x_2 is the distance from the boundary, and U_1 is the local average velocity. Reid assumed $\sigma_2 = 1.3u_*$, and estimated $\tau_2(y)$ from the spatial variation of the turbulent viscosity. For neutral stratification he obtained $\tau_2 = 0.26\,x_2/u_*$.

Wilson, Thurtell & Kidd (1981) showed that (1) and (2) fail when both σ_i and τ_i are allowed to vary with spatial position in that the models predict that fluid particles drift from regions of high to regions of low turbulence. Legg & Raupach (1982) remedied this problem by interpreting the first term on the right-hand side of (1) as a drag force and the second as a randomly varying acceleration. They argued that a mean force needs to be added which arises from the mean pressure gradient that exists in the fluid. For a fully developed flow, the following equation would then be used for the component of the velocity perpendicular to the wall:

$$\mathrm{d}u_2 = -\frac{u_2}{\tau_2}\mathrm{d}t + \alpha_2^{1/2}\mathrm{d}\omega_2 + \frac{\partial\sigma_2^2}{\partial x_2}\mathrm{d}t. \tag{3}$$

Wilson *et al.* (1981) have suggested that a particle trajectory in inhomogeneous turbulence may be viewed as a motion in homogeneous turbulence in transformed coordinates. Durbin (1983, 1984) and Thomson (1984) used this concept to write the following modified form of the Langevin equation for u_2:

$$\mathrm{d}\left(\frac{u_2}{\sigma_2}\right) = -\frac{u_2}{\sigma_2\tau_2}\mathrm{d}t + \left(\frac{2}{\tau_2}\right)^{1/2}\mathrm{d}\omega_2 + \frac{\partial\sigma_2}{\partial x_2}\mathrm{d}t. \tag{4}$$

Wilson *et al.* (1981) showed that the inclusion of $\partial\sigma_2/\partial x_2$ in (4) is equivalent to the use of $\partial\sigma_2^2/\partial x_2$ in (3). They both ensure that a mean force, equal to the mean pressure gradient in the fluid, is included.

Durbin (1984) has examined (2) and (4) for large t/τ_2. His analysis shows that the probability function describing the x_2-coordinate of the displacement is then given as

$$\frac{\partial P}{\partial t} = \frac{\partial}{\partial x_2}\left(K(x_2)\frac{\partial P}{\partial x_2}\right), \tag{5}$$

where $K = \sigma_2^2\tau_2$. If K_2 were not introduced inside the parentheses in (5) a spurious drift would be introduced if $\mathrm{d}K/\mathrm{d}x_2 \neq 0$. Thus, Durbin showed that (2) and (4) introduce a mean drift velocity in a Lagrangian framework that is equal to $\partial(\sigma_2^2\tau_2)/\partial x_2$.

In homogeneous isotropic turbulence $\mathrm{d}\omega_i$ is a Gaussian function with a mean of zero and a variance equal to $\mathrm{d}t$. This is not the case in non-homogeneous turbulence where $\mathrm{d}\omega_i$ is non-Gaussian, even if the Eulerian distribution function for u_1 is Gaussian. Thomson (1984) has developed equations that relate the moments of the random functions appearing in (3) and (4) to the moments of the Eulerian velocity fluctuations and to the spatial variance of the Eulerian turbulence.

The results presented in this paper for computer experiments on dispersion from a point source in a turbulent fluid flowing through a channel are analysed with a modified version of (4). In § 2 a justification is presented for using this form of the Langevin equation. In § 3 the moments of the random function are developed by a more direct method than used by Thomson (1984). This approach has the advantage of emphasizing the approximations that are made in these analyses.

The computer experiments described in § 5 differ from previous studies in that all Eulerian properties of the velocity field are known and that the velocity changes of dispersing fluid particles are directly observed. However, it is not clear how the spatial variation of the time scale, τ_i, can be derived directly from the Eulerian properties of the turbulence. The approach taken is that the analysis is forgiving in specifying this parameter. Some crude assumptions are, therefore, explored. The rationale behind the specification of τ_i is presented in § 4 and in the Discussion Section at the end of the paper.

Most previous applications of the Langevin equation have involved studies of dispersion in the atmospheric boundary layers for which the behaviour in the viscous wall region can be neglected. The computer experiments described in this paper were done at a low enough Reynolds number that a log-layer did not exist, so that the viscous wall region occupies a large part of the channel. The contribution of this paper is that it provides results on Lagrangian statistics under conditions where the non-homogeneities of the velocity field in the viscous wall layer have a significant influence. Furthermore, the success of the modified Langevin equation is tested not only by its ability to predict dispersion in a direction perpendicular to the wall but also by its ability to predict dispersion in the flow direction and the Lagrangian statistics of the velocity field. A motivation is the need to describe the behaviour of wall sources of a scalar contaminant for a range of Schmidt (or Prandtl) numbers and the velocity field seen by solid particles in a turbulent field (Iliopoulos 1998). The possibility of developing a model for the complicated process of aerosol deposition by free flight (Brooke, Hanratty & McLaughlin 1994) is of particular interest.

2. Description of the stochastic method

2.1. *Homogeneous stationary case*

Equation (1) is written as follows by Legg & Raupach (1982):

$$\mathrm{d}u_i = -\frac{u_i}{\tau_i}\mathrm{d}t + \alpha_i^{1/2}\xi_i(t)\mathrm{d}t, \tag{6}$$

where $\mathrm{d}\omega_i = \xi_i(t)\mathrm{d}t$ is a random number sequence that has zero mean, τ_i is a measure of how long the motion persists in the i-direction and α_i is the magnitude of the random fluctuating term. Although (6) is a stochastic difference equation, a solution can be obtained by methods developed for linear ordinary differential equations. For homogeneous isotropic turbulence with $\overline{u_i} = 0$, $\alpha_i = \alpha =$ constant and $\tau_i = \tau =$ constant. The following three properties are postulated (van Kampen 1992):

(i) $\langle \alpha^{1/2}\xi \rangle = 0$ (the average vanishes);

(ii) $\langle \alpha^{1/2}\xi(t)\alpha^{1/2}\xi(t') \rangle = \alpha\delta(t-t')$ (defines the autocorrelation function);

(iii) $\langle \mathrm{d}\omega^2 \rangle = \mathrm{d}t$ (obtained by using Ito calculus and the fact that $\mathrm{d}\omega$ is the increment of a Wiener process).

A term obeying (i), (ii), (iii) is called a Langevin force. Conditions (ii) and (iii) do not completely specify the stochastic process but only its first two moments. The Langevin equation is a prototype of a stochastic differential equation, in that its coefficients are random fluctuations with given statistical properties. The solution of (6) is

$$u_i(t) = u_i(0)\exp(-t/\tau) + \exp(-t/\tau)\int_0^t \exp(t'/\tau)\alpha^{1/2}\xi(t')\mathrm{d}t', \tag{7}$$

where $u_i(t)$ is a fluctuating velocity component and $u_i(0)$ is the value of u_i at time zero. After squaring and averaging for a large number of trajectories the following result is obtained:

$$\langle u_i^2(t) \rangle = \langle u_i^2(0) \rangle \exp(-2t/\tau) + \alpha\tau/2 - \exp(-2t/\tau)\alpha\tau/2, \tag{8}$$

where the brackets signify an ensemble average. In homogeneous stationary turbulence $\langle u_i^2 \rangle = \langle u_i^2(0) \rangle = \sigma^2$, so the coefficient in the Langevin equation is found to be $\alpha = 2\sigma^2/\tau$. Multiplication of (8) by $u_i(0)$ and averaging for a large number of paths

yields

$$\langle u_i(t)u_i(0)\rangle = \sigma^2 \exp(-t/\tau). \tag{9}$$

Thus, the Lagrangian correlation coefficient for a process that obeys the Langevin equation is

$$R_L(t) = \frac{\langle u(0)u(t)\rangle}{\sigma^2} = \exp\left(-\frac{t}{\tau}\right). \tag{10}$$

Since the Lagrangian integral time scale of the fluid, τ_L, is defined as

$$\tau_L = \int_0^\infty R_L(t)\mathrm{d}t \tag{11}$$

it follows that $\tau = \tau_L$. The inexactness of the Langevin equation is reflected in (10), which does not give the correct behaviour for $t \to 0$.

The Langevin equation can thus be written as follows for a homogeneous isotropic field:

$$\mathrm{d}u_i = -\frac{u_i}{\tau_L}\mathrm{d}t + \left(\frac{2\sigma^2}{\tau_L}\right)^{1/2} \mathrm{d}\omega, \tag{12}$$

where $\mathrm{d}\omega = \xi\,\mathrm{d}t$, u_i is the velocity component in the ith-direction, σ is the root mean square of a component of the fluctuating velocity and $\mathrm{d}\omega$ is the increment of the Wiener process.

Equations (3)–(5) can be modified to include the hypothetical case of a homogeneous isotropic field for which σ is constant and τ varies with time, by replacing τ with

$$\tau_A = \frac{1}{t}\int_0^t \tau_L \mathrm{d}t. \tag{13}$$

Then, $\alpha = 2\sigma^2/\tau_A$.

2.2. *Non-homogeneous, stationary turbulence with constant* τ_i

The use of the Langevin equation for homogeneous turbulence is well established. However, the more interesting applications are for non-homogeneous flows. Fully developed turbulent flow in a channel is considered, for which 1, 2, 3 correspond to the streamwise, wall-normal and spanwise coordinates respectively. The mean velocity, U_1, and the root mean squares of the velocity fluctuations, σ_i, vary with x_2. Equation (2) is rewritten as

$$\frac{\mathrm{d}x_i}{\mathrm{d}t} = U_i + u_i, \tag{14}$$

where U_i is the mean velocity defined by Eulerian measurements. For the case considered in this paper, U_i is non-zero for the streamwise direction only.

One approach is to use equation (3) with τ_2, α_2 and ξ_2 being functions of x_2. However, the specification of $\alpha_2 = 2\sigma_2^2/\tau_2$ cannot be justified analytically as is done in § 2.1 for a homogeneous isotropic field. Furthermore, it is not clear that $\langle u_i^2\rangle$ should be the same for all times in a non-homogeneous field and the ensemble average of the velocities of all particles at a given location and time, $\langle u_i^2(x_2)\rangle$, is of more interest, than $\langle u_i^2\rangle$. A desirable condition on the stochastic equation is that at very large times $\langle u_i^2(x_2)\rangle = \sigma_i^2(x_2)$ where σ_i^2 is the Eulerian mean square of u_i. For this reason, the use of a scaled velocity $\langle u_i(u_2)\rangle/\sigma_i(x_2)$, rather than u_i, was an attractive choice for us. At time zero $\langle (u_i/\sigma_i)^2\rangle = 1$.

A stochastic equation similar to (1) can be written as

$$\mathrm{d}\left(\frac{u_2}{\sigma_2}\right) = -\frac{u_2}{\sigma_2\tau_2}\mathrm{d}t + \alpha_2^{1/2}\mathrm{d}\omega_2. \tag{15}$$

If τ_2 is considered to be constant, an analysis similar to what is presented in § 2.1 gives

$$\left\langle \left(\frac{u_2}{\sigma_2}\right)_t^2 \right\rangle = \left\langle \left(\frac{u_2}{\sigma_2}\right)_0^2 \right\rangle \tag{16}$$

for $\alpha_2 = \langle u_2^2/\sigma_2^2\rangle\, 2/\tau_2$, where subscript t signifies time t and subscript 0 signifies time 0. Since $\langle (u_2/\sigma_2)_0^2\rangle = 1$ it follows that $\langle (u_2/\sigma_2)_t^2\rangle = 1$.

Equation (4) introduces into (15) the additional complications of a variable τ_2 and a mean drift defined by the term with $\partial\sigma_2/\partial x_2$. It is not clear that the integration of this equation produces the results given in (16) for all times. However, it might only be necessary that the equation produces the correct behaviour at large times.

The formulation of the Langevin equation both by (1) and (15) indicates a fundamental non-uniqueness. This matter has been discussed by several authors. See, for example, Sawford & Guest (1987) who argue for the use of (15) rather than (1).

3. Properties of the random forcing function for u_i

The method for specifying the random forcing function will now be considered. For homogeneous isotropic turbulence, $\mathrm{d}\omega_i$ is Gaussian with zero mean and variance equal to $\mathrm{d}t$. As already mentioned, $\mathrm{d}\omega_i$ might be non-Gaussian for a non-homogeneous field even if the Eulerian statistics are Gaussian.

This problem is considered by writing the equations for the velocity components measured in a Lagrangian framework in the following form:

$$\mathrm{d}\left(\frac{u_i}{\sigma_i}\right) = -\frac{u_i}{\sigma_i\tau_i}\mathrm{d}t + \mathrm{d}\mu_i, \tag{17}$$

where $\mathrm{d}\mu_i = \alpha_i^{1/2}\mathrm{d}\omega_i$. By taking the ensemble average of (17) the following result is obtained:

$$\langle \mathrm{d}\mu_i\rangle = \left\langle \frac{\mathrm{d}\left(u_i/\sigma_i\right)}{\mathrm{d}t} \right\rangle \mathrm{d}t. \tag{18}$$

Here, and in the remainder of the paper, $\langle\ \rangle$ signifies an ensemble average at a given location, unless specified otherwise. For $i = 2$

$$\frac{\mathrm{d}\left(u_2/\sigma_2\right)}{\mathrm{d}t} = -\frac{u_2}{\sigma_2^2}\frac{\mathrm{d}\sigma_2}{\mathrm{d}t} + \frac{1}{\sigma_2}\frac{\mathrm{d}u_2}{\mathrm{d}t}. \tag{19}$$

For a fully developed flow, $\mathrm{d}\sigma_2/\mathrm{d}t = u_2(\partial\sigma_2/\partial x_2)$ where $(\partial\sigma_2/\partial x_2)$ is the derivative in an Eulerian framework. The substantial derivative is related to Eulerian derivatives as follows:

$$\frac{\mathrm{d}u_i}{\mathrm{d}t} = \frac{\partial u_j u_i}{\partial x_j} + \frac{\partial u_i}{\partial t}. \tag{20}$$

For a stationary field, the substitution of (19) and (20) into (18) gives

$$\langle \mathrm{d}\mu_2\rangle = -\frac{\langle u_2^2\rangle}{\sigma_2^2}\frac{\partial\sigma_2}{\partial x_2}\mathrm{d}t + \frac{1}{\sigma_2}\frac{\partial\langle u_2^2\rangle}{\partial x_2}\mathrm{d}t, \tag{21a}$$

or

$$\langle \mathrm{d}\mu_2 \rangle = \frac{\partial \left(\langle u_2^2 \rangle / \sigma_2 \right)}{\partial x_2} \mathrm{d}t \tag{21b}$$

if the ensemble average of a derivative is assumed equal to the derivative of the ensemble average. If $\langle u_2^2 \rangle$ is approximated by σ_2^2 the drift term in (4) is obtained. If (3) were used $\langle \mathrm{d}\mu_2 \rangle$ is found to be equal to $\partial \sigma_2^2 / \partial x_2$, if $\langle \partial u_2^2 / \partial x_2 \rangle = \partial \sigma_2^2 / \partial x_2$.

Gardiner (1990) and von Kampen (1992) have suggested that it is better to derive equations for the moments directly from the Langevin stochastic differential equation, rather than from a solution of the Langevin equation as is done in § 2.1. Arnold (1974) showed that if a stochastic variable is defined by

$$\mathrm{d}X = f \mathrm{d}t + \mathrm{d}\mu \tag{22}$$

the following relation is valid:

$$\mathrm{d}X^2 = 2Xf \, \mathrm{d}t + 2X \, \mathrm{d}\mu + \mathrm{d}\mu \, \mathrm{d}\mu. \tag{23}$$

This result can be understood by defining a change in $X_1 X_2$

$$\mathrm{d}(X_1 X_2) = X_1(t + \mathrm{d}t) X_2(t + \mathrm{d}t) - X_1(t) X_2(t) \tag{24}$$

with $X(t + \mathrm{d}t) = X(t) + \mathrm{d}X$, so that

$$\mathrm{d}(X_1 X_2) = X_1 \mathrm{d}X_2 + X_2 \mathrm{d}X_1 + \mathrm{d}X_1 \mathrm{d}X_2. \tag{25}$$

If equation (25) with $X_1 = X_2$ is substituted into (24), equation (23) is obtained if terms of higher order than $\mathrm{d}t$ are ignored. The term $\mathrm{d}\mu \, \mathrm{d}\mu$ is kept because $\langle \mathrm{d}\mu \, \mathrm{d}\mu \rangle$ is of order $\mathrm{d}t$.

Applying (23) to (17) gives

$$\mathrm{d}\left(\frac{u_2^2}{\sigma_2^2} \right) = -\frac{2u_2^2}{\sigma_2^2 \tau_2} \mathrm{d}t + 2 \frac{u_2}{\sigma_2} \mathrm{d}\mu_2 + \mathrm{d}\mu_2 \, \mathrm{d}\mu_2. \tag{26}$$

An ensemble average of (26) at some fixed location is taken. From the properties of $\mathrm{d}\mu_2$ it follows that $\langle u_2 \mathrm{d}\mu_2 \rangle = 0$, so that

$$\langle \mathrm{d}\mu_2^2 \rangle = +\frac{2\langle u_2^2 \rangle}{\sigma_2^2 \tau_2} \mathrm{d}t + \frac{1}{\sigma_2^2} \left\langle \frac{\mathrm{d}u^2}{\mathrm{d}t} \right\rangle \mathrm{d}t - \left\langle \frac{2u_2^2}{\sigma_2^3} \frac{\mathrm{d}\sigma_2}{\mathrm{d}t} \right\rangle \mathrm{d}t. \tag{27}$$

Substituting $u_2(\partial \sigma_2 / \partial x_2) = (\mathrm{d}\sigma_2 / \mathrm{d}t)$ and $\langle \mathrm{d}u_2^2 / \mathrm{d}t \rangle = \langle \partial u_2^3 / \partial x_2 \rangle$ gives

$$\langle \mathrm{d}\mu_2^2 \rangle = +\frac{2\langle u_2^2 \rangle}{\sigma_2^2 \tau_2} \mathrm{d}t + \frac{1}{\sigma_2^2} \left\langle \frac{\partial u^3}{\partial x_2} \right\rangle \mathrm{d}t - \frac{2\langle u_2^3 \rangle}{\sigma_2^3} \frac{\partial \sigma_2}{\partial x_2} \mathrm{d}t. \tag{28}$$

Again the ensemble average of a spatial derivative is approximated as the derivative of the ensemble average, so that

$$\langle \mathrm{d}\mu_2^2 \rangle = +\frac{2\langle u_2^2 \rangle}{\sigma_2^2 \tau_2} \mathrm{d}t + \frac{\partial \left(\langle u_2^3 \rangle / \sigma_2^2 \right)}{\partial x_2} \mathrm{d}t. \tag{29}$$

Since $\alpha \mathrm{d}\omega^2 = \mathrm{d}\mu^2$ and $\langle \mathrm{d}\omega^2 \rangle = \mathrm{d}t$ the coefficient α_2 in (15) can be obtained from (29) as

$$\alpha_2 = \frac{2\langle u_2^2 \rangle}{\sigma_2^2 \tau_2} + \frac{\partial \left(\langle u_2^3 \rangle / \sigma_2^2 \right)}{\partial x_2}. \tag{30}$$

Now $\langle \mathrm{d}\mu^2 \rangle$ is the sum of a mean plus a deviation around the mean so that

$$\langle \mathrm{d}\mu^2 \rangle = \langle \mathrm{d}\mu - \langle \mathrm{d}\mu \rangle \rangle^2 + \langle \mathrm{d}\mu \rangle^2. \tag{31}$$

Since $\langle d\mu\rangle^2$ is of order dt^2 (see equation (21)) and $\langle d\mu^2\rangle$ is of order dt (see equation (29)), it follows for small dt that

$$\langle d\mu^2\rangle = \langle d\mu - \langle d\mu\rangle\rangle^2. \tag{32}$$

An equation for $\langle d\mu_2^3\rangle$ can be obtained in the same way as for $\langle d\mu_2^2\rangle$. Let

$$X_1 = \left(u_2/\sigma_2\right)^2, \quad X_2 = \left(u_2/\sigma_2\right). \tag{33}$$

From (17)

$$dX_2 = -\frac{X_2}{\tau_2}dt + d\mu_2. \tag{34}$$

From (25), (33) and (34)

$$dX_2^2 = dX_1 = -\frac{2X_1}{\tau_2}dt + 2X_2 d\mu_2 + \frac{X_1}{\tau_2^2}(dt)^2 - \frac{2X_2 dt\, d\mu_2}{\tau_2} + d\mu_2^2. \tag{35}$$

From (25), (34) and (35) the following relation is obtained if terms of order dt^2 are ignored:

$$dX_1X_2 = -\frac{3X_1X_2}{\tau_2}dt + 3X_1 d\mu_2 - \frac{4X_1 dt\, d\mu_2}{\tau_2} + 3X_2 d\mu_2^2 - \frac{2X_1}{\tau_2}d\mu_2\, dt + d\mu^3. \tag{36}$$

An ensemble average is taken and it is recognized that u_2 is uncorrelated with $d\mu_2$ and that terms with $\langle d\mu_2\rangle dt$ are of order $(dt)^2$:

$$\left\langle d\left(\frac{u_2^3}{\sigma_2^3}\right)\right\rangle = -3\frac{u_2^3}{\tau_2\sigma_2^3}dt + 3\frac{\langle u_2^2\rangle}{\sigma_2^2}\langle d\mu_2\rangle + \left\langle (d\mu_2)^3\right\rangle. \tag{37}$$

Thus

$$\left\langle d\mu_2^3\right\rangle = \frac{\partial\left(\langle u_2^4\rangle/\sigma_2^3\right)}{\partial x_2}dt + \frac{3\langle u_2^3\rangle}{\tau_2\sigma_2^3}dt - \frac{3\langle u_2^2\rangle}{\sigma_2^2}\frac{\partial\left(\langle u_2^2\rangle/\sigma_2\right)}{\partial x_2}dt. \tag{38}$$

An equation for $\langle d\mu_2^4\rangle$ can be obtained by letting

$$X = X_1 = X_2 = (u_2/\sigma_2)^2, \tag{39}$$

where dX is given by (35). From (25) and (35) an equation for $\left\langle d\left(u_4^4/\sigma_2^4\right)\right\rangle$ can be derived, analogous to (37):

$$\left\langle d\mu_2^4\right\rangle = \frac{4\left\langle u_2^4\right\rangle}{\sigma_2^4\tau_2}dt - \frac{4\left\langle u_2^3\right\rangle}{\sigma_2^3}\frac{\partial\left(\langle u_2^2\rangle/\sigma_2\right)}{\partial x_2}dt$$

$$-12\frac{\langle u_2^2\rangle^2}{\sigma_2^4\tau_2}dt - 6\frac{\langle u_2^2\rangle}{\sigma_2^2}\frac{\partial\left(\langle u_2^3\rangle/\sigma_2^2\right)}{\partial x_2}dt + \frac{\partial\left(\langle u_2^5\rangle/\sigma_2^4\right)}{\partial x_2}dt. \tag{40}$$

Changes in the streamwise velocity fluctuations are given by

$$d\left(\frac{u_1}{\sigma_1}\right) = -\frac{u_1}{\sigma_1\tau_1}dt + d\mu_1. \tag{41}$$

The following equations are derived for the moments of $d\mu_1$:

$$\langle d\mu_1\rangle = \frac{\partial\left(\langle u_1u_2\rangle/\sigma_1\right)}{\partial x_2}dt, \tag{42}$$

$$\langle d\mu_1^2\rangle = \left[\frac{2\langle u_1^2\rangle}{\sigma_1^2\tau_1} + \frac{\partial\left(\langle u_1^2u_2\rangle/\sigma_1^2\right)}{\partial x_2}\right]dt, \tag{43}$$

$$\langle \mathrm{d}\mu_1^3 \rangle = \left[\frac{3}{\tau_1} \frac{\langle u_1^3 \rangle}{\sigma_1^3} + \frac{\partial \left(\langle u_1^3 u_2 \rangle / \sigma_1^3 \right)}{\partial x_2} - \frac{3\langle u_1^2 \rangle}{\sigma_1^2} \frac{\partial \left(\langle u_1 u_2 \rangle / \sigma_1 \right)}{\partial x_2} \right] \mathrm{d}t, \tag{44}$$

$$\langle \mathrm{d}\mu_1^4 \rangle = \left[\frac{4\langle u_1^4 \rangle}{\sigma_1^4 \tau_1} - \frac{4\langle u_1^3 \rangle}{\sigma_1^3} \frac{\partial \left(\langle u_1 u_2 \rangle / \sigma_1 \right)}{\partial x_2} - 12 \frac{\langle u_1^2 \rangle^2}{\sigma_1^4 \tau_1} - 6 \frac{\langle u_1^2 \rangle}{\sigma_1^2} \frac{\partial \left(\langle u_1^2 u_2 \rangle / \sigma_1^2 \right)}{\partial x_2} + \frac{\partial \left(\langle u_1^4 u_2 \rangle / \sigma_1^4 \right)}{\partial x_2} \right] \mathrm{d}t. \tag{45}$$

Thompson (1984) derived results for $\overline{\mathrm{d}\mu_2^m}$ by a different approach than used above. Equations (21), (29), (38) and (40) agree with his results if the ensemble averages are replaced by time averages.

Equation (41) gives the change of the values of the fluctuations around the average, not the increment in the instantaneous velocity. Therefore, the change in the mean velocity, at a particular x_2, should be added in order to get the change in the instantaneous streamwise velocity. Using the definition of the substantial derivative and the assumption of a fully developed flow that has only one non-homogeneous direction, x_2, the following equation is obtained for the evolution of the mean streamwise velocity:

$$\frac{\mathrm{d}U_1}{\mathrm{d}t} = \frac{\partial U_1}{\partial x_j} u_j + \frac{\partial U_1}{\partial t} = \left(\frac{\partial U_1}{\partial x_2} \right) u_2, \tag{46}$$

where $(\partial U_1 / \partial x_2)$ is the derivative of the mean Eulerian velocity at x_2.

4. Solution of the Langevin equation

4.1. *Specification of* τ_i

The time scale appearing in the Langevin equation can be rigorously defined only for homogeneous isotropic turbulence. For non-homogeneous turbulence, the integral in (11) need not converge so researchers have interpreted τ_i as the local decorrelation rate, that is the persistence of motion in a certain direction. However its exact definition is unclear. We have followed the lead of previous researchers (Hall 1975; Reid 1979) to estimate the spatial variation of τ_i from the spatial variation of an Eulerian time scale. From numerous studies of wall turbulence one can, therefore, anticipate that τ_i scales with outer variables over most of the channel, $\tau_i u_* / H = f_1(x_2/H)$. Close to the wall τ_i would scale with wall parameters, $\tau_i u_*^2 / \nu = f_2(x_2 u_* / \nu)$. For a large enough Reynolds number a matching region (the log-layer) would exist in which $\tau_i u_* / x_2 = \text{constant}$.

Some guidance in selecting values for τ_i can be obtained from mixing studies in pipes. In a review of such work, Vames & Hanratty (1988) suggested that the measurements can be represented by a constant value of $\tau_2^L = 0.093a/u_*$, where a is the radius of the pipe and u_* is the friction velocity. If the dimensionless half-height of the channel, $H = 150$, is substituted for the pipe radius a, one obtains $\tau_2 u_* / \nu = 14$. However, if the hydraulic radius is used, $\tau_2 u_* / \nu = 28$ is obtained. A dimensionless τ_2 in the neighbourhood of 14–28 seems like a reasonable choice for calculations in which τ_2 is taken constant.

Measurements of spectra of streamwise and normal velocity fluctuations in a channel for a range of Reynolds numbers from 5100 to 48 000, by Warholic (1997), support the suggestion of Vames & Hanratty, in that the median frequency was found to scale approximately with H and u_* for $0.1 < x_2/H < 1$. Lyons (1989) used his direct

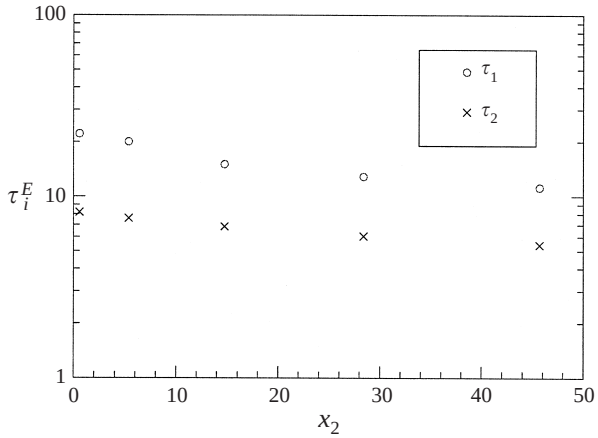

FIGURE 1. Eulerian time-scale dependence on the distance from the wall.

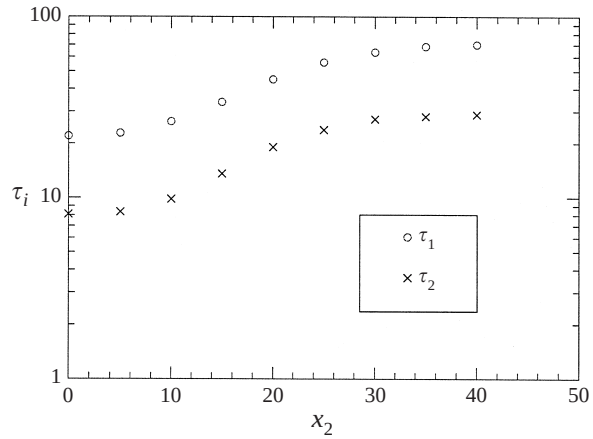

FIGURE 2. Non-Gaussian case: Lagrangian time-scale variation with wall distance.

numerical simulation for turbulent flow in a channel at $H = 150$ to calculate Eulerian temporal correlation coefficients for $x_2 = 0 - 45$. Since the calculations were made over a limited range of times the area under the curve representing the correlation coefficients at a given x_2 could not be calculated. Instead, τ_i^E is defined as twice the value of the time at which R_E is equal to $e^{-1/2} = 0.606$. Eulerian time scales obtained this way are plotted in figure 1. It is noted that τ_1^E is approximately $(2-2.5)\tau_2^E$. More importantly, these Eulerian time scales are found to vary only by a factor of about 2 from $x_2 = 0$ to $x_2 = 45$ for the small Reynolds number used in these calculations. However, one would expect that as $x_2 \to 0$, the length scales characterizing mixing should go to zero. This is consistent with the time scales shown in figure 1 since the velocity fluctuations become quite small for $x_2 \to 0$ and the length scale is the product of a velocity and a time.

The results discussed above were used as a guideline for initial calculations in which a spatially varying τ_i was used. This simply involved the definition $\tau_i = \beta\tau_i^E$, where τ_i^E are the Eulerian time scales given in figure 1 and β is a constant which was selected as equal to 5. Calculations showed that this choice was not satisfactory because it gives

time scales close to the wall which are too large. Consequently, the final calculations were done with the spatially varying time scales shown in figure 2.

This approximation involves the use of a relation which assumes that τ_i can be approximated by constant values (which vary with outer scales) farther away from the wall, and that τ_i equals the Eulerian time scales (which vary with inner variables) in the immediate vicinity of the wall. The rationale for this is that the length scales characterizing the motion (particularly in a direction perpendicular to the wall) are so small that fluid particles are not displaced appreciably over a time period. As a consequence, the Eulerian and Lagrangian time scales are approximately equal.

For the low Reynolds number being considered, the outer region begins at $x_2 = 40$. For $x_2 > 40$, τ_1, τ_2 and τ_3 are, respectively, set equal to 70, 28 and 33. At the wall they are set equal to the Eulerian scales given in figure 1 at $x_2 = 0$. A signoidal curve was used to interpolate between the values specified for small and large x_2.

Finally, it should be pointed out that the use of the assumption that τ_i depends only on local Eulerian time scales appears flawed. In the simple flow field being considered, spatially varying time scales result in a variation of τ_i with time, for a given trajectory, since the particle sees regions which are characterized by different τ_i^E, as it moves around the field. Consequently an attractive hypothesis is to define $\tau_A(t)$ for a given trajectory, by (13). We have found, for the situations considered, that results obtained in this way are not different from those obtained by using $\tau_i(y)$. For simplicity, the effect of previous history on τ_i has been ignored in the calculations.

4.2. *Numerics*

The equation defining the change of velocity along a path is of the form

$$\mathrm{d}u_i = f_i \mathrm{d}t + \mathrm{d}\mu_i' + \langle \mathrm{d}\mu_i \rangle, \tag{47}$$

where $\mathrm{d}\mu_i' = \mathrm{d}\mu_i - \langle \mathrm{d}\mu_i \rangle$. This is solved numerically by specifying a value of u_i at $x_2 = 40$ for $t = 0$. This initial value could be obtained from the Eulerian probability distribution representing u_i at $x_2 = 40$. For the calculations presented in this paper the initial conditions for the model were the same as for the 16 129 paths studied in the computer experiment.

An Adams–Bashforth explicit scheme, that is accurate to second order, was used to solve equation (47). The turbulent velocity of a particle, which was at location x_0 at time zero, was calculated as follows:

$$u_i(\boldsymbol{x}_0, t_{n+1}) = u_i(\boldsymbol{x}_0, t_n) + \tfrac{3}{2}\mathrm{d}u_i(\boldsymbol{x}_0, t_n) - \tfrac{1}{2}\mathrm{d}u_i(\boldsymbol{x}_0, t_{n-1}). \tag{48}$$

A fourth-order Runge–Kutta was tested; the difference was too small to justify the higher computational cost. A Milstein scheme (Kloeden & Platen 1992) was also used, but the results showed no appreciable difference. A well-known difficulty with multistep methods, like the Adams–Bashforth, is that they are not self-starting. In order to extrapolate to the next point information is needed from previous points, which is not normally available at the beginning of the computation. The Euler method, which is first-order accurate and can be viewed as the simplest Runge–Kutta method, was used for the first time step:

$$u_i(\boldsymbol{x}_0, t_{n+1}) = u_i(\boldsymbol{x}_0, t_n) + \frac{\mathrm{d}u_i(\boldsymbol{x}_0, t_n)}{\mathrm{d}t}\Delta t. \tag{49}$$

The same schemes were used to solve the equation of motion to get a new position for the particle:

$$x_i(\boldsymbol{x}_0, t_{n+1}) = x_i(\boldsymbol{x}_0, t_n) + [\tfrac{3}{2}u_i(\boldsymbol{x}_0, t_n) - \tfrac{1}{2}u_i(\boldsymbol{x}_0, t_{n-1})]\Delta t. \tag{50}$$

Again, for the first time step, an Euler scheme is used:

$$x_i(\boldsymbol{x}_0, t_{n+1}) = x_i(\boldsymbol{x}_0, t_n) + u_i(\boldsymbol{x}_0, t_n)\Delta t. \tag{51}$$

In general, the probability density function of the random irregular term is not Gaussian. The selection of the random number in (47) needs to take this into account. This is achieved by using a method developed by Baerensten & Berkowicz (1984). Two Gaussian distributions, that have means of $\mu\imath_1$ and $\mu\imath_2$ and variances of σ^2, are summed with different weights. The probability of selecting a number from $N(\mu\imath_1, \sigma\imath^2)$ is p and from $N(\mu\imath_2, \sigma\imath^2)$ is 1-p, so that

$$\mathrm{d}\mu = pN(\mu\imath_1, \sigma\imath^2) + (1-p)N(\mu\imath_2, \sigma\imath^2). \tag{52}$$

To $O(\mathrm{d}t)$, the average value of $\mathrm{d}\mu$ is 0. Parameters $\mu\imath_1, \mu\imath_2, \sigma\imath^2$ and p are functions of the distance from the wall, x_2. They are selected so as to satisfy the following equations which are accurate to first order of $\mathrm{d}t$:

$$p\mu\imath_1 + (1-p)\mu\imath_2 = 0, \tag{53a}$$

$$p(\mu\imath_1^2 + \sigma\imath^2) + (1-p)(\mu\imath_2 + \sigma\imath^2) = \langle \mathrm{d}\mu^2 \rangle, \tag{53b}$$

$$p(\mu\imath_1^3 + 3\mu\imath_1\sigma^2) + (1-p)(\mu\imath_2^3 + 3\mu\imath_2\sigma\imath^2) = \langle \mathrm{d}\mu^3 \rangle, \tag{53c}$$

$$p(\mu\imath^4 + 6\mu\imath_1^2\sigma\imath^2 + \sigma\imath_1^4) + (1-p)(\mu\imath^4 + 6\mu\imath_2^2\sigma\imath^2 + \sigma\imath_2^4) = \langle \mathrm{d}\mu^4 \rangle. \tag{53d}$$

Since $\langle \mathrm{d}\mu_i^m \rangle$ is $O(\mathrm{d}t)$ for all values of m, the selected random numbers, $\mathrm{d}\mu_i$, could satisfy conditions of higher order than given in (53). However, this is not practical since Eulerian data are not available to evaluate higher-order moments. One could argue that it is meaningless to use $\langle \mathrm{d}\mu_i^m \rangle$ up to $m = 4$ and that only the specification of $\langle \mathrm{d}\mu_i^2 \rangle$ can be justified. Our reason for considering $\langle \mathrm{d}\mu_i^3 \rangle$ and $\langle \mathrm{d}\mu_i^4 \rangle$ is to examine the effects of the skewness and flatness of the velocity fluctuations, which can be quite large close to the wall.

The Gaussian distributions $N(\mu\imath_1, \sigma\imath^2)$ and $N(\mu\imath_2, \sigma\imath^2)$ are specified by selecting random numbers in the interval [0,1). By using the Box–Muller transformation (Press *et al.* 1989), the outcome was changed into a Gaussian deviate. The Box–Muller scheme was chosen over the Brent transformation (Press *et al.* 1989) because it can be much faster on parallel machines (Convex 1990).

The uniform random number generator that was used is a standard function of the mlib mathematical library of the HP-Convex Company. All uniform random number generators suffer from the drawback that the sequence produced is repeated after a certain number of steps. In order to avoid this problem in a single run and have the maximum period possible, an integer *8 (the maximum length of an integer that can be accommodated by the machine) was used to seed the uniform random number generator. Then the period of the sequence was 2^{64}.

5. Results of computer experiments

5.1. *Description of the computer experiments*

All of the results are presented in a non-dimensional form, using the friction velocity and the kinematic viscosity. The system considered is fully developed turbulent flow between two smooth walls, separated by a distance $2H$, that extend to infinity in

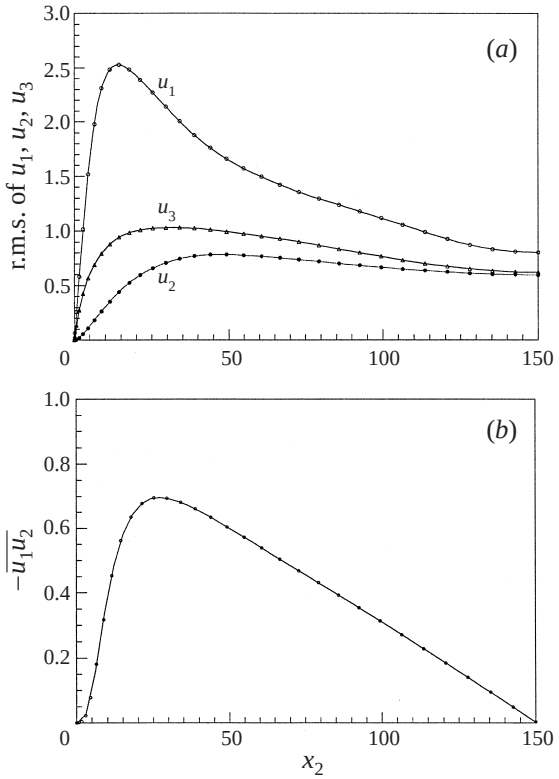

FIGURE 3. Plots of the root-mean-square velocity components (*a*), and Reynolds stress (*b*) $x_2 = 0$ is the bottom wall and 150 is the centreline.

the streamwise and spanwise directions. The space between the plates is filled with a fluid flowing at a Reynolds number of 4520 based on the average fluid velocity and the distance between the plates, $2H$. Dimensionless H has a value of 150. The three-dimensional, time-dependent, fluctuating velocity field is obtained by solving numerically the Navier–Stokes equations on a three-dimensional grid, as described by Lyons, Hanratty & McLaughlin (1991). Calculated values of the mean squares of the velocity components and of the Reynolds shear stress are given in figure 3. Skewness and flatness factors, plotted in figure 4, are used to evaluate $\langle \mathrm{d}\mu_i^3 \rangle$ and $\langle \mathrm{d}\mu_i^4 \rangle$. The straight horizontal lines represent Gaussian behaviour. Large departures are noted, so a consideration of the effects of skewness and flatness in specifying $\mathrm{d}\mu_i$ is of interest.

Fluid particles that were released at a distance $x_2 = 40$ from the bottom wall were tracked in time in the flow field. The position of each particle was continuously updated by numerically integrating its equation of motion in time:

$$\frac{\partial x_i(x_0, t_n)}{\partial t} = V_i(x_0, t_n). \tag{54}$$

The velocity of the particle at some later time, $t + \Delta t$, is the velocity determined by the DNS at $x_i + \Delta x_i, t + \Delta t$. The method for tracking fluid particles is an extension of the algorithm developed by Kontomaris (1991).

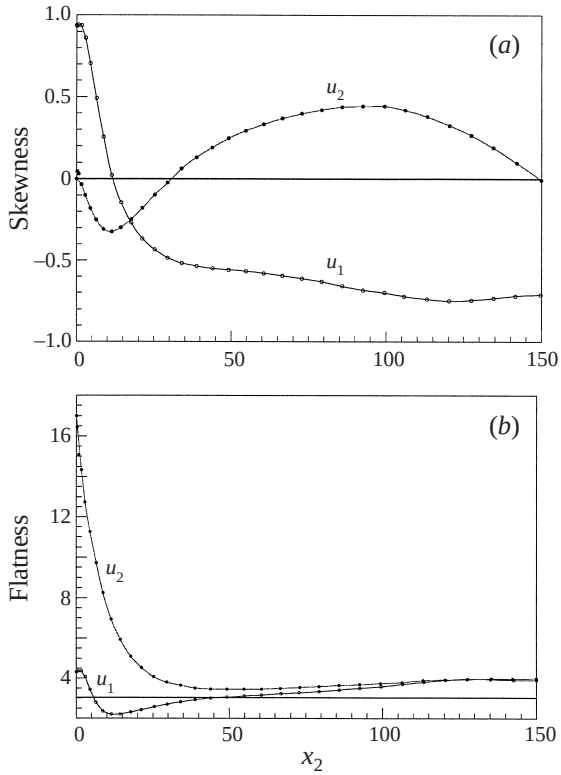

FIGURE 4. Plots of the velocity skewness (*a*), and velocity flatness (*b*) from the DNS. 0 is the bottom wall, 150 the centreline. The straight lines show a Gaussian behaviour.

5.2. *Results of computer experiments*

Concentration profiles obtained from the computer experiments are shown in figures 5–8 as data points. The curves are solutions of the Langevin equations. The particles spread as a cloud in the x_1-, x_2- and x_3-directions. The abscissa, x_2, is the dimensionless distance from the wall. The channel is divided into 30 bins equally spaced in the x_2-direction. The number of particles in each bin is divided by the volume to give the concentration. Averages over x_1 and x_3 are taken at fixed x_2.

At $t = 0$ all the particles are at $x_2 = 40$. Over the period $t = 0$–20 the particles spread symmetrically. The root-mean-squared displacement increases roughly as the product of the root mean square of the normal velocity fluctuations at $x_2 = 40$ and the time. As time increases, the profile becomes more asymmetric, in that particles spread to larger distances in the positive x_2-direction. Particles moving to the wall region see smaller velocities and move shorter distances when they reverse their direction. As a consequence, the maximum in the concentration profile moves closer to the wall. The calculations suggest that for larger times a broad maximum will exist at the wall. It is expected that this maximum would decrease with increasing time. At large enough time the particles would be uniformly spread over the channel section.

Averages of the concentration over x_2 and x_3, from the computer experiment, are presented as a function of x_1 and of time in figure 9. Again for $t = 0$–20 the particles spread symmetrically in the x_1-direction. As time proceeds, particles diffuse into the region close to the wall, where the mean velocity in the x_1-direction is smaller than

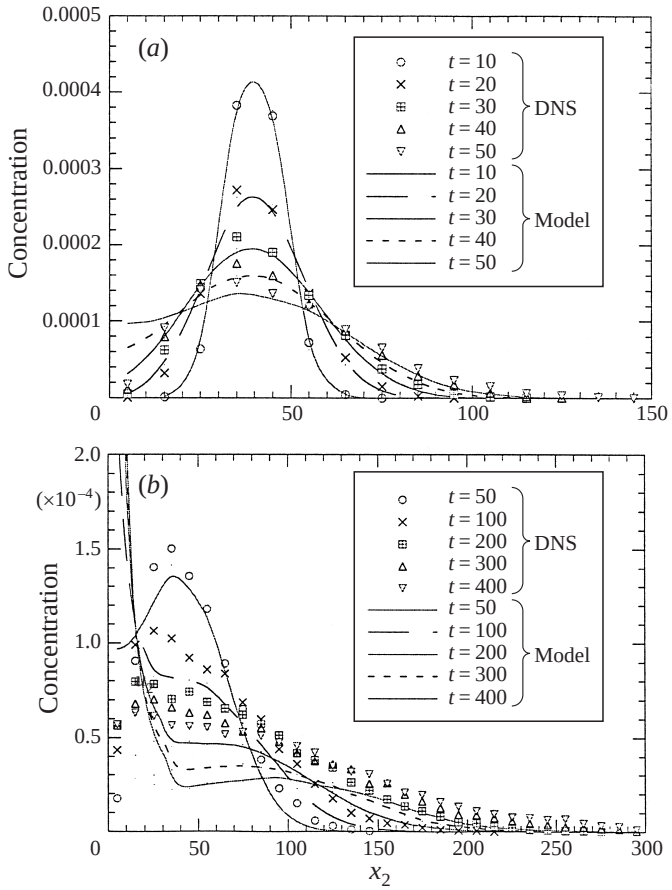

FIGURE 5. Comparison between concentration profiles of fluid particles at (*a*) small and (*b*) large times for case 1 (table 1). $x_2 = 0$ is the bottom wall and 300 is the top wall. The symbols are results from the DNS and the lines results from the model.

in the central region. As a result, the concentration profiles show a large tail, whose extent, at a given time, depends on profiles in the x_2-direction at earlier times. The peak in the profile is convected downstream at a velocity of $c = 15.8$, which is roughly equal to the bulk velocity, $U_b = 15.4$.

Values of the ensemble average of the mean square of the velocity fluctuations in the normal direction, $\langle u_2^2 \rangle^{1/2}$, are shown in figure 10. The curve represents the Eulerian values of σ^2. At $t = 0$, $\langle u_2^2 \rangle^{1/2} = \sigma_2$ and all the particles are at $x_2 = 40$. For small times, particles with larger velocities are displaced larger distances from $x_2 = 40$. As a result, the intensity at $x_2 = 40$ drops below the Eulerian value. The profile of $\langle u_2^2 \rangle$ around $x_2 = 40$ tends to be asymmetric because the skewnesses at $x_2 > 30$ are positive. Particles that are close to the wall are seen to adjust more rapidly to the local Eulerian values than the particles at larger distances from the wall. At very large times the Lagrangian and Eulerian values are equal. Values of $\langle u_2^3 \rangle$ are presented in figure 11. Again, it is seen that these are not equal to $\overline{u_2^3}$, the solid curve. The very large values of positive skewness for the Lagrangian velocities arise because the region of large x_2 is populated by particles which had a large u_2 at $t = 0$. Close to the wall $\langle u_2^3 \rangle$ adjusts to $\overline{u_2^3}$ more rapidly than in the central region of the channel.

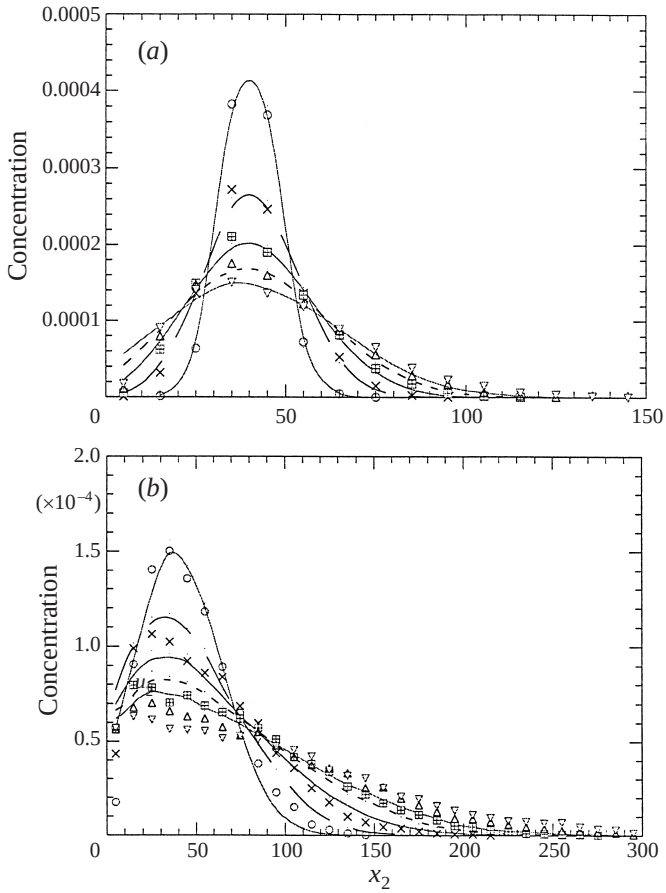

FIGURE 6. As figure 5 but for case 2 (table 1).

Correlation coefficients, defined as $R_{ii} = \langle u_i(t)u_i(0)\rangle/\sigma_i(0)\sigma_i(t)$, are given in figure 12. It should be noted that the ensemble average in this case is for all the particles in the field at a given time; that is, particles at all x_2 locations are included in the average. The correlation coefficient decays to zero much faster for the normal velocity fluctuations than for the streamwise velocity fluctuations. The time scale, defined as twice the value of the time t at which the Lagrangian correlation coefficient is equal to $e^{-1/2} = 0.606$, gives values of $\tau_1 = 70$, $\tau_2 = 28$ and $\tau_3 = 33$. A comparison with the results for τ_1^E at $x_2 = 40$, given in figure 1, reveals that both τ_1/τ_2 and τ_1^E/τ_2^E are approximately equal to 2.2.

6. Results of the stochastic model

6.1. *Outline*

The stochastic equation that is used to calculate a possible change of the fluctuating velocity components u_i along a fluid particle trajectory is

$$\mathrm{d}\left(\frac{u_i}{\sigma_i}\right) = -\frac{u_i}{\sigma_i\tau_i}\mathrm{d}t + \bar{A}_i\mathrm{d}t + \mathrm{d}\mu_i, \tag{55}$$

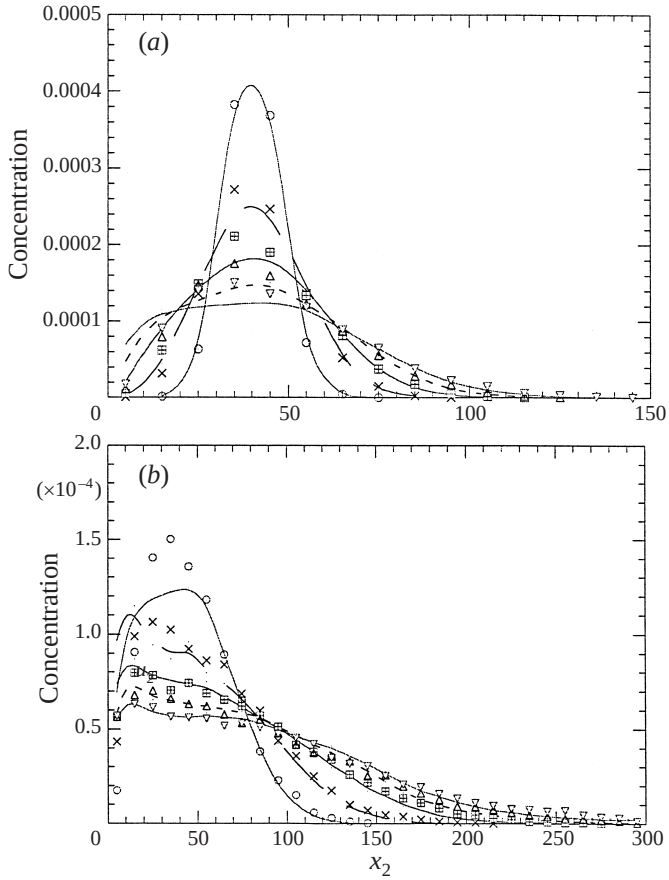

FIGURE 7. As figure 5 but for case 3 (table 1).

where $\bar{A}_i \mathrm{d}t$ represents $\langle \mathrm{d}\mu_i \rangle$, $\mathrm{d}\mu_i$ is a random variable with a mean of zero, and repeated indices do not imply summation. In all of the calculations the ergodic approximation is used so that the ensemble average at a given x_2 (denoted by $\langle\ \rangle$) is replaced by Eulerian time averages (denoted by an overbar), obtained from the DNS by Lyons (1989). Thus

$$\langle A_1 \rangle = \bar{A}_1 = \frac{\partial \left(\dfrac{\overline{u_1 u_2}}{\sigma_2} \right)}{\partial x_2}, \tag{56}$$

$$\langle A_2 \rangle = \bar{A}_2 = \frac{\partial \sigma_2}{\partial x_2}, \tag{57}$$

$$\langle A_3 \rangle = \bar{A}_3 = 0. \tag{58}$$

Values of $\sigma_1(x_2), \sigma_2(x_2), \overline{u_1 u_2}(x_2)$ are given in figure 3.

Table 1 summarizes the conditions for which results of calculations are presented. For the cases in which a Gaussian distribution was explored, $\mathrm{d}\mu_i$ is given by a Gaussian distribution, with a variance $\langle \mathrm{d}\mu_1^2 \rangle = 2\mathrm{d}t/\tau_i$. When a non-Gaussian distribution was used the moments of $\mathrm{d}\mu_2$ were defined from (29), (38), (40) by replacing the ensemble averages with the time averages. Because measurements of the gradient of the fifth

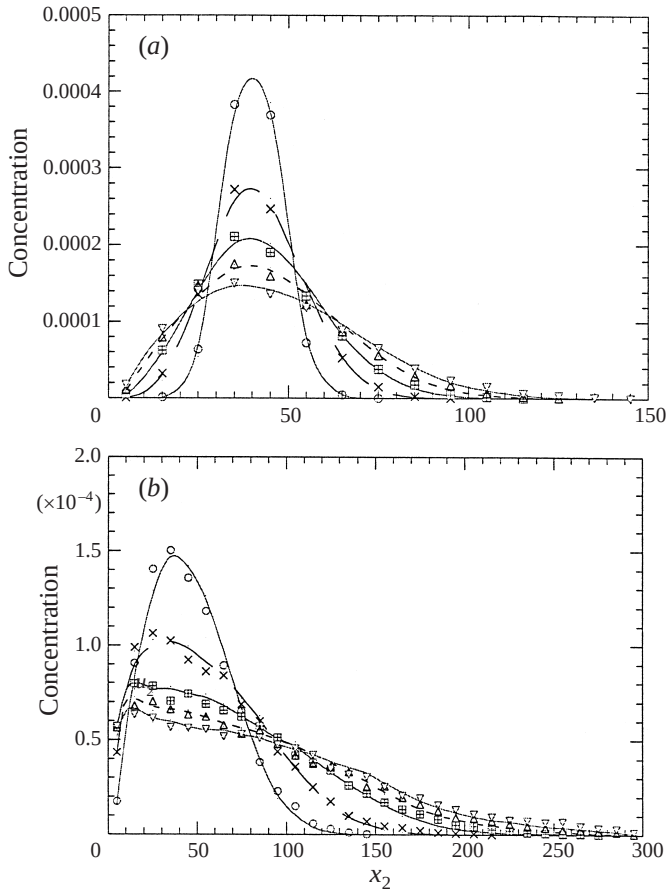

FIGURE 8. As figure 5 but for case 4 (table 1).

Case	τ_1	$\bar{A}_i$	Random forcing
1	$\tau_1 =$ constant $\tau_2 =$ constant	$\bar{A}_i = 0$	Gaussian
2	$\tau_1 =$ constant $\tau_2 =$ constant	$\bar{A}_i \neq 0$	Gaussian
3	$\tau_1 =$ constant $\tau_2 =$ constant	$\bar{A}_i \neq 0$	Non-Gaussian
4	$\tau_1 \neq$ constant $\tau_2 \neq$ constant	$\bar{A}_i \neq 0$	Non-Gaussian

TABLE 1. Value of the parameters for different runs of the stochastic model.

moment of the velocity are not available the third term on the right-hand side of (40) was set equal to zero. The moments of $\mathrm{d}\mu_1$, obtained from (43), (44), (45), again are obtained by replacing ensemble averages with time averages. Terms $\overline{u_1^2 u_2}, \overline{u_1^3 u_2}, \overline{u_1^4 u_2}$ were set equal to zero since data for these quantities are not available. Justification for this is obtained from DNS calculations of $\partial\left(\langle u_1^2 u_2\rangle/\sigma_1^2\right)/\partial y$. These are found to

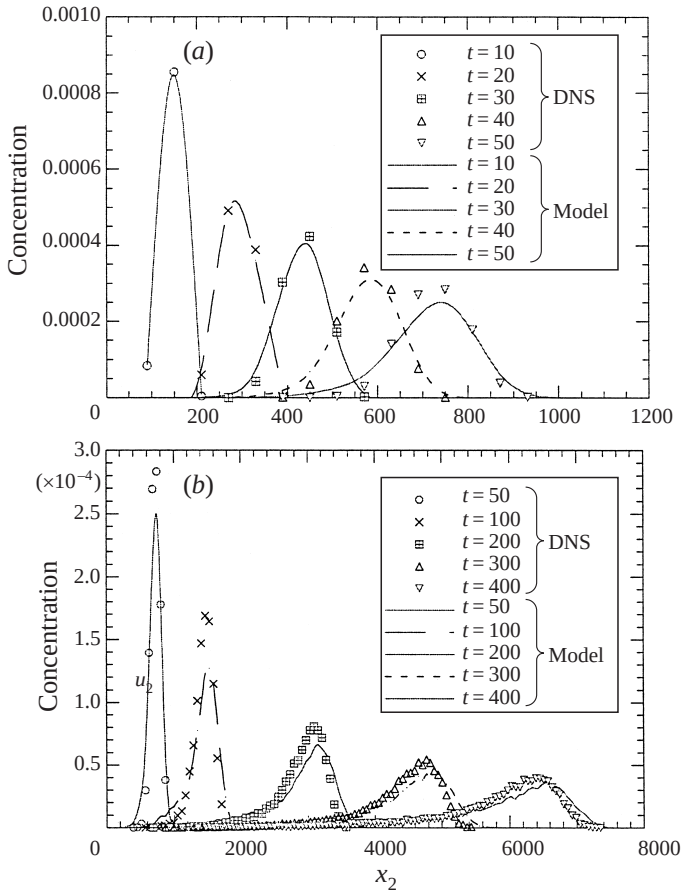

FIGURE 9. Comparison between streamwise dispersion of fluid particles for case 4 at (*a*) small and (*b*) large times. $x_1 = 0$ is the initial location of the particles. The symbols are results from the DNS and the lines results from the model.

be close to zero. The terms $\partial\left(\langle u_1^3 u_2\rangle/\sigma_1^3\right)/\partial x_2$ and $\partial\left(\langle u_1^4 u_2\rangle/\sigma_1^4\right)/\partial x_2$ are expected to be less important.

6.2. *Case* 1: $\tau_2 = 28, \bar{A}_i = 0$, *Gaussian forcing function*

Figure 5 compares calculated concentration profiles at different dimensionless times with measurements from the DNS. The model calculations were done for $\tau_2 = 28$, and $\bar{A}_i = 0$. The random term $\mathrm{d}\mu_i$ was defined by a Gaussian distribution. The turbulent intensities (root-mean-square fluctuating velocities, σ_i) are not constant but a function of the distance from the walls. If a particle hit the wall (an infrequent happening) it was bounced off through an elastic collision, (no flux).

Good agreement between the model and the experiments is observed for $t = 10$ and $t = 20$. For larger t the model predicts an accumulation of particles at the wall, which is not observed in the calculations with the DNS.

6.3. *Case* 2: $\tau_2 = 28, \bar{A}_i \neq 0$, *Gaussian forcing function*

The only difference between case 2 and case 1 is that the parameters $\bar{A}_i$ appearing in (56) are not equal to zero. They are now defined by (57) and (58). As indicated in §§ 1 and 3, these are included to oppose the tendency of particles to drift from regions

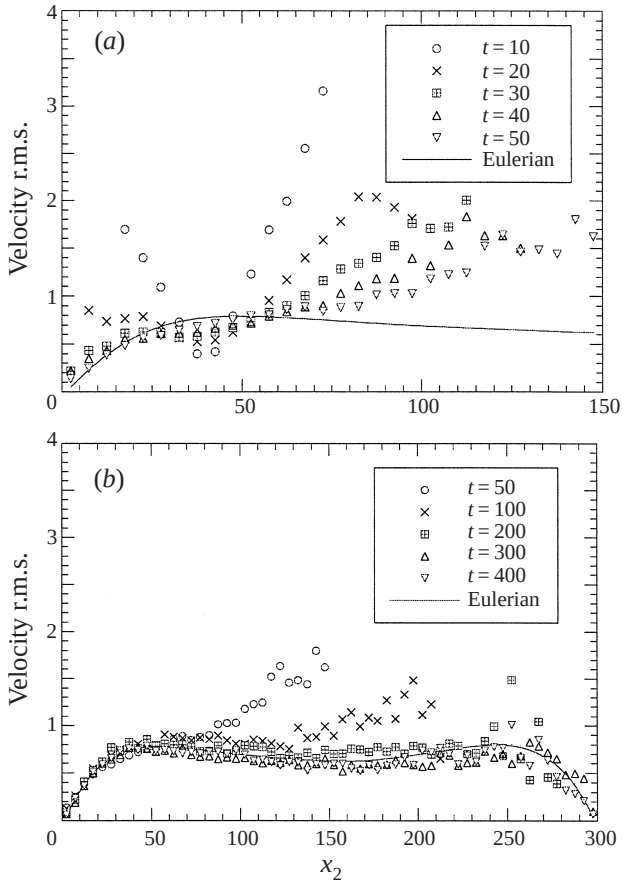

FIGURE 10. Intensity of normal fluid velocity fluctuations obtained from the DNS at (*a*) at small times and (*b*) at large times.

of high turbulence to regions of low turbulence; that is, they allow for a pressure gradient in the fluid to oppose the drift. Figure 6 shows calculated concentration profiles. An improvement is noted over case 1 at large times. The fluid particles do not accumulate at the bottom wall and more particles spread toward the centreline. However the model overpredicts the dispersion for $x_2 < 40$ and underpredicts it for $x_2 > 40$.

6.4. *Case* 3: $\tau_2 = 28, \bar{A}_i \neq 0$, *non-Gaussian forcing function*

Case 3 differs from case 2 in that the p.d.f. of the random term is not Gaussian: it has both skewness and flatness. It should be noted that the values of the third and fourth moments of the random term are not the Eulerian skewness and flatness.

The inclusion of skewness and flatness improves the agreement between the DNS and the model, as shown in figure 7. The particles, now, spread farther away towards the top wall. For large times ($t > 100$), the model is in good agreement with the computer experiment throughout the channel. For intermediate times ($30 < t < 50$) the model overpredicts the dispersion: the peaks of the profiles obtained from the model are low compared to the peaks obtained from calculations with the DNS. It should be noted that in this case none of the particles actually reached the walls.

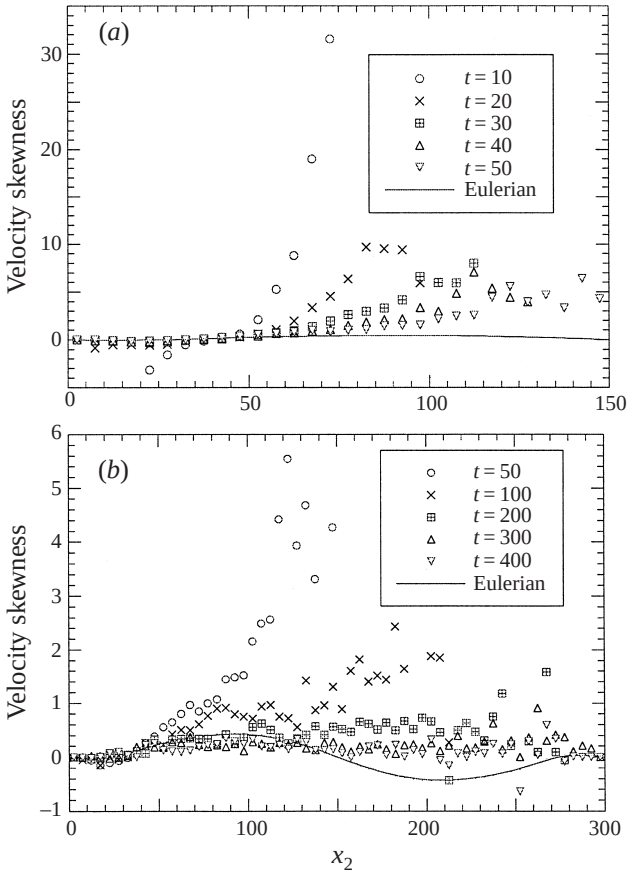

FIGURE 11. Skewness of normal velocity fluctuations obtained from the computer experiments (*a*) at small times and (*b*) at large times.

6.5. *Case* 4: $\tau_i \neq$ *constant*, $\bar{A}_i \neq 0$, *non-Gaussian forcing function*

The calculations considered in cases 1, 2 and 3 illustrate the need to consider drift terms, $\bar{A}_i$, and to include effects associated with skewness and flatness of the velocity fluctuations. Further improvements require a consideration of the influence of the time scales, τ_i, which are not known *a priori*.

Different values for the normal time scale, τ_2, than used in case 3 were explored. A value half that used for cases 1, 2 and 3, that is $\tau_2 = 14$, produces no difference in the calculated concentrations profiles from $t = 0$ until $t = 15$. This suggests that the spread for small times is dictated mainly by the initial values of the velocities of the particles. Differences in calculations from case 3 were noted for $t > 15$, in that better agreement was noted close to the wall between the calculated concentration profiles and the profiles obtained from the DNS. When the larger time scale was used, $\tau_2 = 28$, the agreement was improved in the centre of the channel. These results showed that the assumption of a constant time scale, τ_2, needs to be abandoned if better results are desired. In particular, smaller values of τ_2 need to be used close to the wall.

A reasonable approach is to assume that τ_1 and τ_2 are proportional to the Eulerian time scales obtained from temporal autocorrelations and from frequency spectra. This

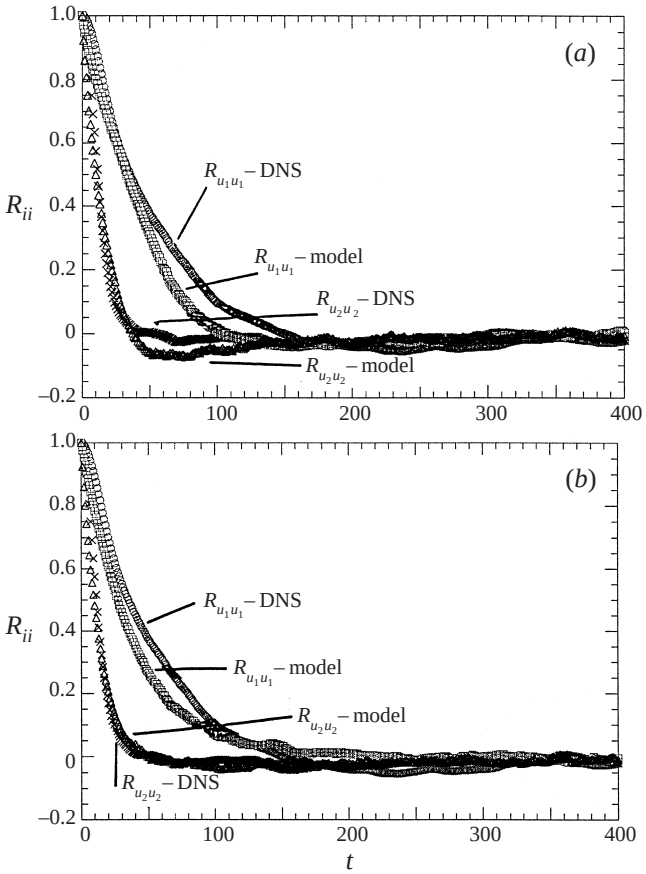

FIGURE 12. Comparison between fluid velocity correlation graphs over time, (*a*) for case 2 and (*b*) for case 4.

was pursued in the thesis by Iliopoulos (1998). This gives larger time scales close to the wall than in the centre regions of the channel and, therefore, a poorer agreement than obtained for case 3. As discussed in § 4.1, this led to the use of the functions for τ_i shown in figure 2.

Figure 8 compares concentration profiles obtained from the DNS and the model calculations for case 4. Very good agreement is noted. For small times the shapes of the concentration profiles are exactly the same. For intermediate times, the particles approach the bottom wall, but do not have a tendency to accumulate there. The shape of the profiles is the same at $t = 50$, where a significant difference was noted for case 3. For large t the model does not overpredict results from the DNS, as it did at $t = 400$ around $x_2 = 40$ for cases 1, 2 and 3. Figure 13 gives values of the ensemble averages $\langle u_2^2 \rangle^{1/2}$ calculated from the stochastic model for case 4. Very good agreement is noted with the computer results in figure 10. For small times the model not only predicts correctly that the intensities deviate from the Eulerian values, but it also gives the correct values. The main reasons for the scatter is that the bins at large x_2 have few particles and that the skewness is affecting the behaviour in this region. The predictions of the skewness of the normal velocity fluctuations with the stochastic model for case 4 (in figure 11) are also in very good agreement with the

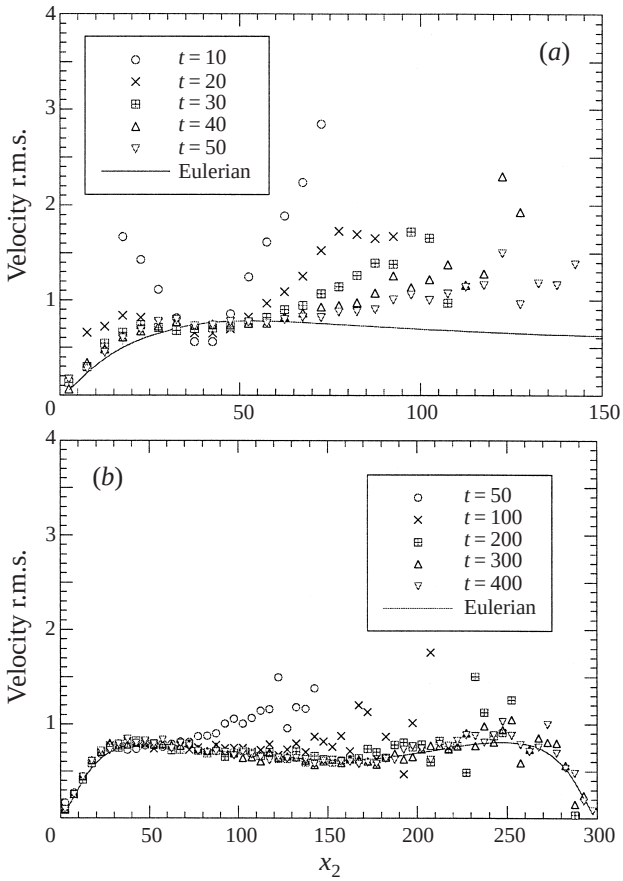

FIGURE 13. Intensity of normal fluid velocity fluctuation obtained from the model case 4, (*a*) at small times and (*b*) at large times.

results of the DNS experiment in figure 14. At small times the model predicts the trend and the values of the skewness, surprisingly well. For longer times the model is still quite satisfactory.

Calculated concentration profiles in the streamwise direction are compared with results obtained with the DNS. These profiles are a more severe test of the accuracy of the model than the ones in figure 8, because streamwise positions are very sensitive to the previous history of the particles. Therefore, one can see a slight difference between the DNS and the model. It is more noticeable in the peaks and in the tails of the clouds after $t = 50$.

Figure 12 compares calculations of Lagrangian correlations for the normal and streamwise velocity fluctuations for cases 2 and 4. The velocity correlations in figure 12(*a*) compare results from the DNS and the model calculations for case 2. In figure 12(*b*) the comparison is made between the DNS and the model calculation for case 4. It should be noted that the ensemble average is for all the particles in the field. The calculated normal velocity correlation for case 2 drops below the data from the DNS experiment. This could result from the selection of a time scale that is too large for the region below $x_2 = 40$. The particles start at $x_2 = 40$ and some of them move towards the bottom wall. The persistence of their motion in the normal direction increases

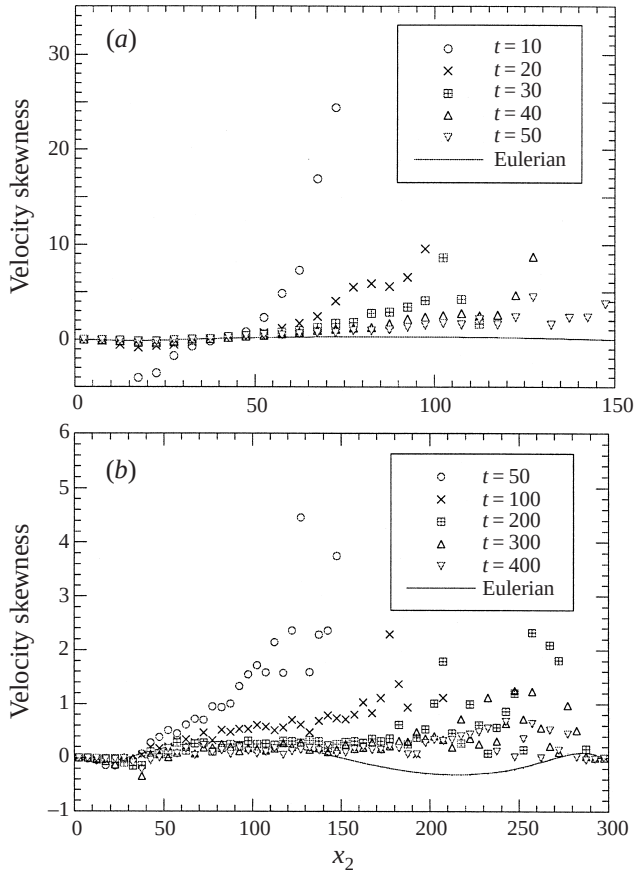

FIGURE 14. Skewness of normal velocity fluctuations obtained from model case 4, (*a*) at small times and (*b*) at large times.

with increasing τ_2. As pointed out earlier, the time scale near the wall is overestimated in case 2. This could also explain why the model for case 2 overpredicts concentrations close to the wall. Another possible source of error is the Gaussian assumption. The Eulerian skewness profile across the channel, figure 3, shows that the skewness is negative below $x_2 = 40$ and positive above $x_2 = 40$. Since the particles are released at $x_2 = 40$, the assumption of a Gaussian behaviour causes the correlation to overshoot zero at intermediate times, for which the population for $x_2 < 40$ is overpredicted. A comparison of figures 12(*a*) and 12(*b*) shows that calculations based on case 4 produce better agreement with the DNS experiments than do calculations based on case 2. The inability of the model calculations to capture the correct behaviour close to $t = 0$ reflects a limitation of the Markovian assumption.

7. Discussion

This paper uses studies of the dispersion of fluid particles in a DNS of turbulent channel flow to test theories that have been developed to apply the Langevin equation to non-homogeneous fields. The particular case that is examined is a point source at $x_2 = 40$, where x_2 is the distance from the wall made dimensionless with wall

parameters. The agreement between the Langevin models and the calculations with the DNS is quite good.

All of the statistical parameters of the turbulence used in the model, with the exception of the time scales, were obtained from Eulerian properties of the field. In this sense, the Langevin equation relates Lagrangian properties of the turbulence to Eulerian properties. For the case considered, the Eulerian time scales, such as those obtained from spectra or correlations, vary by only a factor of four from the centre of the channel to the wall. Therefore, we felt justified to carry out calculations that use constant time scales.

These confirmed previous studies which showed that particles tend to move from regions of high turbulence to regions of low turbulence. The inclusion of a mean drift in the forcing term in the Langevin equation is needed to counteract this effect (as suggested by a number of previous researchers). This term can be interpreted as a time-mean pressure gradient which is related to spatial variation of the Reynolds stresses.

The calculations with a constant time scale also reveal the need to take into consideration the non-Gaussian properties of the turbulent field. The skewness of the velocity fluctuations in the normal direction is positive outside the viscous wall region and negative inside. Because of this, particles moving away from the point source, at $x_2 = 40$, toward the centreline can have larger positive velocities than is predicted with a Gaussian distribution. Likewise, particles moving toward the wall will have larger negative velocities. Consequently, the extent of the dispersion is larger than predicted with a Gaussian distribution. This is seen in figure 6 where the values of the maxima are predicted to be too large for $t = 100 - 400$. The time constants used in this calculation are Lagrangian scales; they are larger than the Eulerian time constants, such as shown in figure 2 for $x_2 > 40$.

Further improvements to the calculations required a consideration of the spatial variation of the time scales. One approach would be to assume that they vary with the distance from the wall in the same way as the Eulerian time scales and are larger by a factor of about four. This does not improve the results, which are worse than for case 3 where the time scales were kept constant. Consideration of figure 7 shows that, for intermediate times, $t = 40$–100, the model for case 3 predicts large concentrations of particles close to the wall that are not observed in the DNS experiments. This behaviour has been explained as being the result of the use of a time scale that is too large close to the wall. A physical explanation is that particles moving toward the wall persist in their motion for too long a time period. This led to the argument that the Lagrangian time constants are equal to the Eulerian time constants right at the wall.

Calculations using this assumption agree with experiments done in a DNS, apart from a slight disagreement in the calculation of concentration profiles in the streamwise direction. This comparison is a severe test because dispersion in the streamwise direction is strongly dependent on the mean streamwise velocities that the particles saw during the period that they were followed. Therefore $c(x, t)$ reflects the accuracy with which concentration profiles in a direction perpendicular to the wall have been predicted at previous times.

The understanding of the influence of spatially varying time constants emerges as a central problem. One of the questions that arises is how to introduce this variation into the Langevin equation. This paper simply substitutes $\tau_i(y)$ for a constant τ_i. (However, as pointed out in § 2, the previous history of a particle might have to be taken in to account.) From previous studies of wall turbulence, one can assume

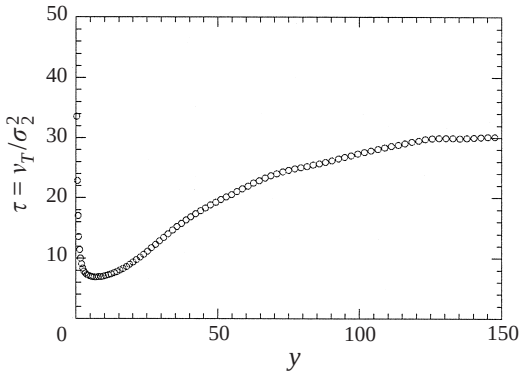

FIGURE 15. Time scale defined from the ratio of σ_2^2 and the dissipation of turbulent energy.

that τ_i scales with wall parameters in the viscous wall region and with outer flow parameters in the outer region. An increase in Reynolds number would, therefore, be accompanied by an increase in the ratio of the scales in the centre of the channel to the scales at the wall. From experience in scaling mean velocities, the matching of scaling relations for the outer region to scaling relations in the viscous wall layer could involve a 'log-layer' assumption in which τ_i would depend only on y and u_*. The Reynolds number was so small, for the case considered in this paper, that no log-layer existed. Therefore a simple matching was used.

The main conclusion is that recent equations developed by Thomson (1984) and Durbin (1983, 1984) to introduce influences of non-homogeneities into the Langevin equation produce a good stochastic representation of the dispersion of fluid particles. For an accurate representation, though, information is required not only on the higher-order moments of the velocity distribution (namely skewness and flatness), but also on the variation of the Lagrangian time scale in the flow field. Clearly, more work needs to be done on this problem.

One possibility is to use the local turbulent viscosity, v_T. Figure 15 presents the ratio of v_T to σ_2^2, made dimensionless with wall parameters. It is noted that there is a very rough similarity between this time scale and the values of τ_2 shown in figure 2. Clearly, this is a possible alternative to the approach suggested in figure 2.

This work is supported by the NSF under grant NSF CTS 95-03000 and by the DOE under grant DOE DEFG02-86ER13556. Computer measurements have been provided by the National Center for Supercomputer Applications (NCSA), Urbana, IL.

REFERENCES

ARNOLD, L. 1974 *Stochastic Differential Equations.* Wiley Interscience.

BAERENTSEN, J. H. & BERKOWICZ, R. 1984 Monte Carlo simulation plume dispersion in the convective boundary layer. *Atmos. Environ.* **18**, 701.

BROOKE, J. W., HANRATTY, T. J. & MCLAUGHLIN. J. B. 1994 Free-flight mixing and deposition of aerosols. *Phys. Fluids* **6**, 3404.

CONVEX 1990 *Convex Mathematical Library and Vector Library, User's Guide*, 5th Edn. Convex Computer Corporation, Richardson, TX.

DURBIN, P. A. 1983 Stochastic differential equations and turbulent dispersion. *NASA Reference Publi.* 1103.

Durbin, P. A. 1984 Comments on papers by Wilson *et al.* (1981) and Legg and Raupach (1982). *Boundary-Layer Met.* **29**, 408.

Eckelman, L. D. & Hanratty, T. J. 1972 Interpretation of measured variations of the eddy conductivity. *Intl J. Heat Mass Transfer* **15**, 2231.

Gardiner, C. W. 1990 *Handbook of Stochastic Methods.* Springer.

Hall, C. D. 1975 The simulation of particle motion in the atmosphere by a numerical random walk model. *Q. J. R. Met. Soc.* **101**, 235.

Hanratty, T. J. 1956 Heat transfer through a homogeneous isotropic turbulent field. *AIChE J.* **2**, 359.

Hanratty, T. J. 1958 Note on the analogy between momentum transfer and heat or mass transfer for a homogeneous isotropic turbulent field. *AIChE J.* **4**, 495.

Hanratty, T. J. & Flint, D. L. 1958 Velocity profile for fully developed turbulent flow in a pipe. *AIChE J.* **2**, 132.

Iliopoulos, I. 1998 A stochastic Lagrangian model for non-Gaussian fluid turbulence and its application to describe particle dispersion in a channel. PhD thesis, University of Illinois, Urbana, IL.

Kampen, N. G. van 1992 *Stochastic Processes in Physics and Chemistry*. North Holland Elsevier.

Kloeden, P. E. & Platen, E. 1992 *Numerical Simulation of Stochastic Differential Equations*, ch. 10. Springer.

Kontomaris, K. 1991 Point source dispersion in a direct numerical simulation of turbulent channel flow. PhD thesis, University of Illinois, Urbana, IL.

Legg, B. J. & Raupach, M. R. 1982 Markov chain simulation of particle dispersion in non-homogeneous flows. *Boundary-Layer Met.* **24**, 3.

Lyons, S. L. 1989 A direct numerical simulation of fully developed turbulent channel flow with passive heat transfer. PhD thesis, University of Illinois, Urbana, IL.

Lyons, S. L., Hanratty, T. J. & McLaughlin, J. B. 1991 Large-scale computer simulation of fully developed turbulent channel flow with heat transfer. *Intl J. Numer. Meth. Fluids* **13**, 999.

Obukhov, A. M. 1959 Description of turbulence in terms of Lagrangian variables. *Adv. Geophys.* **6**, 113.

Papavassiliou, D. V. & Hanratty, T. J. 1995 The use of Lagrangian methods to describe turbulent transport of heat from a wall. *Indust. Engng Chem. Res.* **34**, 3359.

Papavassiliou, D. V. & Hanratty, T. J. 1997 Transport of a passive scalar in a turbulent channel flow. *Intl J. Heat Mass Transfer.* **40**, 1303.

Press, W. H., Flannery, B. P., Teukolsky, S. A. & Vetterling, W. T. 1989 *Numerical Recipes, The Art of Scientific Computing*, Cambridge University Press.

Reid, J. D. 1979 Markov chain simulations of vertical dispersion in the neutral surface layer for surface and elevated releases. *Boundary-Layer Met.* **16**, 3.

Sawford, B. L. & Guest, F. M. 1987 Lagrangian stochastic analysis of flux-gradient relationships in the convective boundary layer. *J. Atmos. Sci.* **44**, 1152.

Taylor, G. I. 1921 Diffusion by continuous movements. *Proc. Lond. Math. Soc.* **20**, 196.

Taylor, G. I. 1935 Statistical theory of turbulence. *Proc. Lond. Math. Soc.* **151**, 421.

Thomson, D. J. 1984 A random walk modelling of diffusion in non-homogeneous turbulence. *Q. J. R. Met. Soc.* **110**, 1107.

Vames, J. S. & Hanratty, T. J. 1988 Turbulent dispersion of droplets for air flow in a pipe. *Exps. Fluids* **6**, 94.

Warholic, M. D. 1997 Modification of turbulent channel flow by passive and addictive devices. PhD thesis, University of Illinois, Urbana, IL.

Wilson, J. D., Thurtell, G. W. & Kidd, G. E. 1981 Numerical simulation of particle trajectories in inhomogeneous turbulence. Part 2. Systems with variable turbulent velocity scale. *Boundary-Layer Met.* **21**, 423.